Paired stable isotopes (O, C) and clumped isotope thermometry of magnesite and silica veins in the New Caledonia Peridotite Nappe

Benoît Quesnel, Philippe Boulvais, Pierre Gautier, Michel Cathelineau, Cedric M. John, Malorie Dierick, Pierre Agrinier, Maxime Drouillet

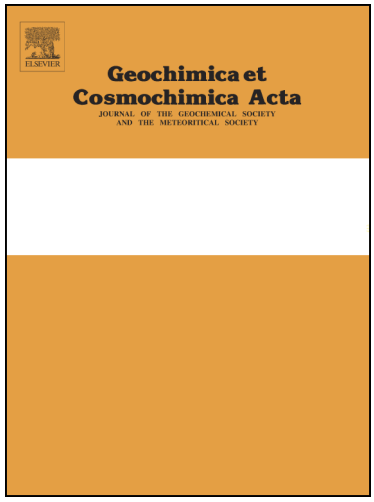

Paired stable isotopes (O, C) and clumped isotope thermometry of magnesite and silica veins in the New Caledonia Peridotite Nappe

Benoît Quesnel, Philippe Boulvais, Pierre Gautier, Michel Cathelineau, Cédric M. John, Malorie Dierick, Pierre Agrinier, Maxime Drouillet

PII: S0016-7037(16)30130-2
DOI: http://dx.doi.org/10.1016/j.gca.2016.03.021
Reference: GCA 9677

To appear in: *Geochimica et Cosmochimica Acta*

Received Date: 11 September 2015
Accepted Date: 21 March 2016

Please cite this article as: Quesnel, B., Boulvais, P., Gautier, P., Cathelineau, M., John, C.M., Dierick, M., Agrinier, P., Drouillet, M., Paired stable isotopes (O, C) and clumped isotope thermometry of magnesite and silica veins in the New Caledonia Peridotite Nappe, *Geochimica et Cosmochimica Acta* (2016), doi: http://dx.doi.org/10.1016/j.gca.2016.03.021

Paired stable isotopes (O, C) and clumped isotope thermometry of magnesite and silica veins in the New Caledonia Peridotite Nappe

Benoît Quesnel*, Philippe Boulvais, Pierre Gautier

Géosciences Rennes, Université Rennes1, UMR 6118 CNRS, 35042 Rennes Cedex, France: benoitquesnel@hotmail.fr, philippe.boulvais@univ-rennes1.fr, pierre.gautier@univ-rennes1.fr

Michel Cathelineau

Université de Lorraine, CNRS, CREGU, GeoRessources Lab., 54506 Vandoeuvre-les-Nancy, France : michel.cathelineau@univ-lorraine.fr

Cédric M. John

Department of Earth Science and Engineering and Qatar Carbonate and Carbon Storage Research Centre (QCCSRC), Imperial College London, Prince Consort Road, London SW7 2AZ, UK. cedric.john@imperial.ac.uk

Malorie Dierick, Pierre Agrinier

Institut de Physique du Globe de Paris, Sorbonne Paris Cité, Univ Paris Diderot, UMR 7154 CNRS, F-75005 Paris, France. dierick@ipgp.fr, agrinier@ipgp.fr

Maxime Drouillet

Service géologique, Konimbo Nickel SAS, 98883 Voh, New Caledonia. mdrouillet@koniambonickel.nc

** corresponding author*

Keywords: Peridotite, weathering, magnesite, silica, stable isotopes, clumped isotope thermometry, laterite, low temperature hydrothermalism.

Abstract

The stable isotope compositions of veins provide information on the conditions of fluid-rock interaction and on the origin of fluids and temperatures. In New Caledonia, magnesite and silica veins occur throughout the Peridotite Nappe. In this work, we present stable isotope and clumped isotope data in order to constrain the conditions of fluid circulation and the relationship between fluid circulation and nickel ore-forming laterization focusing on the Koniambo Massif. For magnesite veins occurring at the base of the nappe, the high $\delta^{18}O$ values between 27.8‰ and 29.5‰ attest to a low temperature formation. Clumped isotope analyses on magnesite give temperatures between 26°C and 42°C that are consistent with amorphous silica - magnesite oxygen isotope equilibrium. The meteoric origin of the fluid is indicated by calculated $\delta^{18}O_{water}$ values between -3.4‰ to +1.5‰ Amorphous silica associated with magnesite or occurring in the coarse saprolite level displays a narrow range of $\delta^{18}O$ values between 29.7‰ and 35.3‰. For quartz veins occurring at the top of the bedrock and at the saprolite level, commonly in association with Ni-talc-like minerals, the $\delta^{18}O$ values are lower, between 21.8‰ and 29.0‰ and suggest low-temperature hydrothermal conditions (~40-95°C). Thermal equilibration of the fluid along the geothermic gradient before upward flow through the nappe and/or influence of exothermic reactions of serpentinization could be the source(s) of heat needed to form quartz veins under such conditions.

1. INTRODUCTION

Carbonate and silica veins occur in various geological contexts, and are the marker of past geological fluid circulation. Understanding the conditions of veins formation is of primary importance to decipher the role of fluids in the transfer of heat and matter, the transport and deposition of metals, and the mechanical properties of shear zones and faults. Stable isotopes are one of the historical tools used in the characterization of fluid-rock interactions (Urey, 1947; McCrea, 1950; Epstein et al., 1953; Emiliani, 1966; Craig and Boato, 1955). Theoretically, stable isotopes give access to the fluid stable isotopic composition and the temperature of precipitation of minerals. However, estimates of temperature and fluid composition are interdependent. That is the reason why stable isotopes studies have to be undertaken with a strong knowledge

of the local geology and in association with complementary methods of fluid characterization, like fluid inclusions studies or other geothermometers.

The recent development of the carbonate clumped isotope thermometer has rapidly been considered as a very promising tool in Earth Sciences (Eiler, 2007). This method is based on the thermodynamic phenomenon of "clumping" which consists in the preferential bonds formation between the heavy isotopes of carbon and oxygen in carbonate minerals. Unlike conventional carbonate thermometers, the clumped isotope thermometer allows temperatures of formation of carbonate to be estimated independently of the initial fluid isotopic composition. By extension, it can provide an estimate of the $\delta^{18}O$ value of the parent fluid since the $\delta^{18}O$ of the carbonate and temperatures are measured independently on the same aliquot of sample.

For the last two decades, the study of carbonate and silica veins developed in ultramafic rocks has attracted a renewed interest given the implications of this process for permanent carbon capture and storage through CO_2 mineralization (Kelemen and Matter, 2008; Kelemen et al., 2011; Oelkers et al., 2013; Ulrich et al., 2014), and in the understanding of lateritic nickel ore formation (Butt and Cluzel, 2013 and references herein). The New Caledonia Peridotite Nappe hosts one of the largest lateritic nickel ore deposit representing around 30% of the global reserves in nickel, thus making New Caledonia the 7th nickel producer in the world. In New Caledonia as in many other places worldwide (Caribbean, South America, Balkans, Russia, West Africa, South East Asian, Australia) Ni-laterites result from the intense weathering of ultramafic rocks exposed at the surface under hot and humid climate. Their development requires the dissolution of protolith minerals leading to i) the export of soluble elements and ii) the in-situ authigenesis of mineral phases hosting the insoluble elements. In the case of peridotites in New Caledonia, Si and Mg are exported whereas the laterites are enriched in iron oxi-hydroxides. Ni, with an intermediate behavior, is concentrated at the base of the lateritic profile where it reaches economic concentrations as Ni-bearing goethite (Trescases, 1975; Freyssinet, 2005). The erratic nickeliferous high-grade ore is located along fractures; it is known as garnierite, a mix of Ni-rich serpentine, Ni talc-like minerals and Ni-sepiolite (e.g. Faust, 1966; Brindley and Hang, 1973; Villanova-de-Benavent et al., 2014; Cathelineau et al., 2015b; Fritsch et al., in press) commonly associated with silica.

In New Caledonia (Fig. 1), numerous magnesite ($MgCO_3$), quartz and amorphous silica veins occur at different levels in the peridotite nappe and are thought to represent by-products of the laterization process (Glasser, 1904; Trescases, 1975). A *per descensum* model of fluid circulation was proposed in which Si and Mg are exported downward along fractures cutting through the nappe (Trescases, 1975).

Many studies have concentrated on the mineralogical characterization of the Ni bearing phases (Brindley and Hang, 1973; Villanova-de-Benavent et al., 2014; Cathelineau et al., 2015b; Dublet et al., 2015; Fritsch et al., in press), but only few studies focused on the understanding of the physical and chemical conditions of Si, Mg and Ni mobility. Based on stable isotope analyses ($\delta^{18}O$) of Ni talc-like minerals in garnierite from Morocco (Bou Azzer), Ducloux et al (1993) showed that they could form between 25ºC and 100ºC. Part of this large spread in temperature is due to uncertainties in the oxygen isotope fractionation factors between Ni talc-like minerals, Ni serpentine-like minerals and water. These authors consider that this temperature range is consistent with a low temperature hydrothermal origin.

For silica occurrences from New Caledonia, Saboureau and Trichet (1978) focused on fluid inclusions included in quartz. They identified two generations of quartz, respectively crystallized at <30ºC and >120ºC. Unfortunately, these samples were collected in soils and represent transported relicts of dismantled quartz occurrences. It is consequently difficult to place them in their genetic context. Recently, Fritsch et al (in press) invoked conditions of low-temperature hydrothermalism to explain the succession of Ni-bearing phases filling fractures and ending with quartz. A temperature of about 70°C is estimated for quartz precipitation by analogy with quartz formed in sandstones.

For magnesite formed via carbonation of peridotite variously serpentinized, on the basis of stable isotopes analyses (C and O), most authors argue that carbonation occurs at low temperature and that the fluid is of meteoric origin but rarely propose to link carbonation and laterization processes (Oman: Kelemen et al., 2011; Streit et al., 2012; West California: Barnes et al., 1973; Poland: Jedrysek and Halas, 1990; Balkans: Fallick et al., 1991; Jurkovic et al., 2012; Greece: Gartzos, 2004; East Australia: Oskierski et al., 2013; New Caledonia: Quesnel et al., 2013). On the other hand, some authors argue that few carbonation events likely occurred at hydrothermal conditions on the basis of stable isotopes analyses (Balkans: Fallick et al., 1991;

Norway: Beinlich et al., 2012) and clumped isotope thermometry (Oman: Falk and Kelemen, 2015).

In this study, we perform stable isotopes analyses on magnesite and silica veins and clumped isotope analyses on magnesite veins from New Caledonia, with a special attention to the Koniambo massif (Fig. 1,2) where the recent development of a mining site allows the access to numerous and exceptional outcrops. We show how the two isotopic methods are complementary and can help to constrain the conditions of veins formation. We also question the *per descensum* model of fluid circulation proposed to explain the vertical distribution of the different mineralization in the peridotite nappe.

2. GEOLOGICAL SETTING

New Caledonia is located in the southwest Pacific Ocean, 1300 km east of Australia (Fig. 1). Peridotites are abundant on the island as a consequence of the Eocene obduction of a sliver of oceanic lithosphere (Cluzel et al., 2012). The Peridotite Nappe sub-horizontally overlies the substratum which is comprised of several volcano sedimentary units (Cluzel et al., 2012). The New Caledonian Peridotite Nappe is exposed in the "Massif du Sud" and as a series of klippes along the northwestern coast (Fig. 1).

Laterite occurs at the top of the peridotites (Fig. 1). Several planation surfaces attest to distinct episodes of weathering and/or epeirogenic movements during the Cenozoic (Latham, 1986; Chevillotte et al., 2006; Sevin et al., 2012). Capping the laterite profile, a ferricrete composed of indurated iron oxides (hematite) mainly occurs as relicts 1 to 2 m thick. Below the ferricrete, the limonitic level is mainly composed of oxi-hydroxides (goethite) and reaches about 20 m in thickness. In this level, the structure of the rock is totally erased. At the base of the profile, the saprolitic level consists in an intermediate state of alteration between limonite and the underlying peridotite. This level reaches around 30m thick. The highly fractured structure of the protolith is preserved. The saprolite level hosts a diffuse Ni mineralization as well as an erratic nickeliferous high-grade ore (Cathelineau et al., 2015a and b; Fritsch et al., in press), known as garnierite veins.

Garnierite occurs as fracture infillings and consists in an association of Ni-rich serpentine and Ni talc-like minerals often associated with silica (Trescases, 1975;

Cluzel and Vigier, 2008; Cathelineau et al., 2015b). Some garnierite occurrences formed syn-tectonically (Cluzel and Vigier 2008) and occur occasionally as hydraulic breccia where silica cement hosts clasts of serpentine and Ni talc-like minerals (Myagkiy et al., 2015). Fractures can also be filled solely by silica.

Beneath the saprolite, the main part of the nappe consists of peridotites in which no silica occurs. Peridotites are highly fractured. Serpentinization is intensive in the deformed zones. At the base of the nappe, peridotites are pervasively serpentinized and highly sheared, constituting the so-called Serpentine Sole.

The sole hosts numerous magnesite veins (Quesnel et al., 2013) commonly associated with amorphous silica (Ulrich et al., 2014). Elsewhere in New Caledonia, silica also occurs as infillings of late normal faults of regional extent, as pervasive silicification at the base of the nappe, locally known as the "Mur de silice" and as veins spatially associated to the Saint Louis and Koum Oligocene granitoid intrusions (Paquette and Cluzel, 2007; Jacob, 1985; Aye et al., 1986).

These occurrences are not studied here as they do not relate to the supergene alteration system of the Koniambo Massif. This massif (Fig. 2) corresponds to one of the klippen occurring along the northwestern coast (Fig. 1). As everywhere on the island, the nappe is capped by a highly dissected and partly reworked lateritic profile (Maurizot et al., 2002). At lower elevations, laterites of the westerly-dipping Kaféaté plateau probably belong to a younger planation surface (Latham, 1977; Chevillotte et al., 2006).

3. Sampling and Samples

3.1 Strategy

In the Koniambo massif, a recently opened mining site allows the sampling of the Peridotite Nappe nearly continuously from the Serpentine Sole to the lateritic profile (Quesnel et al., 2016). The Serpentine Sole is well exposed along cross-sections several hundreds of meters long and a few tens of meters high. The intermediate levels of the Nappe can be observed along an access road reaching the summit of the mining face where mining operations presently expose the laterite and the transition to the fractured peridotite. The veins have been collected at all levels in the Peridotite Nappe in order to get information on the circulation of fluids at the nappe scale

(~800m thick) on the 1D vertical direction. On each sampling site (Fig. 2), the nature of the structure hosting veins has been described when possible.

To obtain a first estimate on the representativeness of the Koniambo Massif with regards to the whole New Caledonia Peridotite Nappe, some samples have been collected at other locations within New Caledonia (Fig. 1): magnesite veins in the nearby Kopéto Massif (Foué peninsula and Koné), quartz veins from the coarse saprolite level from Thio Plateau and Monéo and amorphous silica from Népoui.

3.2 Magnesite

In the Koniambo massif, magnesite occurs mainly as veins in the Serpentine Sole (Fig. 3a, b). Some magnesite veins occur along fractures up to a few hundred of meters above this level (sampling sites 3 and 5, Fig. 2 and Table 1). In many cases, magnesite veins display a cauliflower texture which attests of a non-oriented growth. Some occurrences show a coarse fibrous texture where fibers of monomineralic magnesite are orthogonal to vein walls (Fig. 3b,c). At the Serpentine Sole level, magnesite veins occur preferentially within and along the margins of meter-thick low-dipping shear zones that are also marked by the development of serpentine (Fig. 3a,b). These veins are locally folded or offset by subsidiary shear planes (Fig. 3a). Most of the veins occurring outside the main shear zones have an orientation and coarse fibrous texture suggestive of tension gashes opened during the same shear regime (Fig. 3b,c; see also Quesnel et al., 2013). In soils (Fig. 3d), magnesite appears as nodules that can reach a few tens of cm in width. In general, magnesite samples are mono-mineralic but locally intimately associated with amorphous silica at the Serpentine Sole level.

3.3 Quartz veins and amorphous silica

Quartz and amorphous silica samples have been examined using optical and electronic microscopies (MEB), and the nature of silica polymorphs has been checked by Raman spectroscopy. In the coarse saprolite level and the underlying bedrock, quartz veins occur as fractures infillings. These infillings correspond to the re-opening of ancient fractures commonly filled by serpentine, and in some cases by nickel-rich (or nickel-bearing) serpentine and/or talc-like minerals (Fig. 4c,d,f). They can occur as large branched networks of veins (Fig. 4a), as massive veins (Fig. 4c) or as thin

films (Fig. 4d). Locally, quartz occurs as brown micro-crystalline quartz infillings (Fig. 4b, f; " Mic Qz" in Table 1), generally preceding the clearer yellow, whitish to clear quartz (Fig. 4b, c, d f; "Qz" in Table 1). The brown color is due to the presence of micron-size inclusions of goethite and hematite. Raman analyses of these various types of quartz show systematically three main bands around 130 cm^{-1}, 205 cm^{-1} and 465 cm^{-1}.

Two types of amorphous occurrences were studied: i) brown opal occurs as very late coating or drapery-like on blocks of the coarse saprolite level, which constitutes a rather rare case, (Fig. 4e; "brown opal" in Table 1); ii) translucent opal closely associated with magnesite at the Serpentine Sole, as micro-spherule (Koniambo; Fig. 4g,h; first three rows in Table 1) or as microfracture infillings (Nepoui). Raman analyses show a large band between 300 and 500 cm^{-1} and in some case a band at 460 cm^{-1}.

Similar quartz opal samples were collected in other New Caledonian occurrences for comparison (Fig. 1 and Table 1).

4. Analytical techniques

4.1 Oxygen and carbon isotopes in magnesite

The isotopic analysis of 21 magnesite samples has been performed at the stable isotope laboratory of the University of Rennes 1, France. Samples were finely crushed in a boron carbide mortar, then reacted with anhydrous phosphoric acid at 75ºC for 24h. The experimental fractionation factor between magnesite and CO_2 is $\alpha_{CO2\text{-}Magnesite}$=1.009976 at 75ºC (Das Sharma et al., 2002). CO_2 was analyzed on a VG OPTIMA triple collector mass spectrometer. In the absence of magnesite standard, in-lab calcite standard (Prolabo Rennes) samples were analyzed together with the magnesite samples under identical conditions in order to control the general reliability of the protocol. The analytical uncertainty is estimated at ±0.3‰ for oxygen and ±0.2‰ for carbon by duplication of several analyses. The results are reported using the δ notation relative to VSMOW for O and to VPDB for C.

4.2 Magnesite clumped isotopes

The clumped isotope value of a carbonate sample can be deducted by measuring CO_2 following acidification, and using the Δ_{47} notation (in ‰) that compares the abundance of the rare ^{13}C-^{18}O bonds within a sample relative to a calculated stochastic distribution (Eiler and Schauble, 2004; Affek and Eiler, 2006):

$$\Delta_{47} = \left[\frac{R^{47}}{2R^{13} \cdot R^{18} + 2R^{17} \cdot R^{18} + R^{13} \cdot \left(R^{17}\right)^2} - \frac{R^{46}}{2R^{18} + 2R^{13} \cdot R^{17} + \left(R^{17}\right)^2} - \frac{R^{45}}{R^{13} + 2R^{17}} + 1 \right] \cdot 1000 \quad (1)$$

The Δ_{47} value is calculated from the measured ratios (R^i) of masses 45, 46 and 47 to mass 44 and by calculating R^{13} ($^{13}C/^{12}C$) and R^{18} ($^{18}O/^{16}O$) from R^{45} and R^{46} assuming random distribution. R^{17} is calculated from R^{18} assuming a mass-dependent relationship between ^{18}O and ^{17}O. The higher the Δ_{47} is, the lower the temperature of formation of the mineral (e.g. Ghosh et al. 2006).

Clumped isotope analyses were performed on 7 samples of magnesite in the Qatar Stable Isotopes Laboratory at Imperial College, London, UK. Magnesite was finely crushed and samples of ~5 mg were digested online in a common acid bath composed of 105% ortho-phosphoric acid at 90ºC during 1 hour. The liberated CO_2 gas was continuously trapped and purified by passage through a conventional vacuum line with multiple cryogenic traps and Porapak-Q trap held at -35ºC (Dennis and Shrag, 2010) and was analyzed using a Thermo Finnigan MAT-253 gas source mass spectrometer. The analysis protocol followed procedures described by Huntington et al. (2009) and Dennis et al. (2011) comprising measurements that consisted of 8 acquisitions with 7 cycles per acquisition and an integration time of 26 s. Each cycle included a peak center, background measurements and an automatic bellows pressure adjustment aimed at a 15V signal at mass 44. The sample gas was measured against an Oztech reference gas standard ($\delta^{13}C$ =-3.63 ‰ VPDB, $\delta^{18}O$ =-15.79 ‰ VPDB). Each sample was measured at least three times using separate aliquots to improve counting statistics. An internal standard (Carrara marble, “ICM”, 0.312‰), a published inter-laboratory standard ("ETH3", Meckler et al., 2014, 0.634‰ before acid fractionation correction) and heated gases were analyzed regularly in order to correct for non-linearity (Huntington et al., 2009) and to transfer the measured values in the absolute reference frame (Dennis et al., 2011). Finally, an acid fractionation

factor of 0.069‰ was added to the Δ_{47} values in the absolute reference frame to account for acid fractionation at 90ºC (Guo et al., 2009, Wacker et al., 2013). The analytical uncertainties of the Δ_{47} measurements were added by Gaussian error propagation using standard error of the mean.

4.3 Oxygen isotopes in quartz veins and amorphous silica

The isotopic analysis of 26 silica samples has been performed at the stable isotope laboratory of Institut de Physique du Globe de Paris, France. Samples were finely crushed and reacted with BrF_5 as an oxidizing agent overnight in Ni tubes at 550ºC following the method of Clayton and Mayeda (1963). O_2 was directly analyzed on a Thermo-Fisher Delta V mass spectrometer. During the course of the analyses, the measurements of 14 NBS28 quartz standard allowed to control the general reliability of the protocol (mean = 9.67 ± 0.1 ‰, n= 14).

Thirteen other silica samples have been analyzed at the stable isotope laboratory of Géosciences Rennes (University of Rennes 1, France). Samples were and finely crushed and O_2 was liberated from minerals through reaction with BrF5 at 670°C overnight following the method of Clayton and Mayeda (1963). O_2 was then converted into CO_2 by reaction with hot graphite. Isotopic ratios were measured on a VG SIRA 10 triple collector. NBS 28 quartz standard and in-house A1113 granite standard were routinely analyzed together with samples; the analytical uncertainty is ±0.2‰. The O isotope composition is reported using the δ notation relative to VSMOW.

5. RESULTS

5.1 Magnesite

The stable isotopes compositions of magnesites (Fig. 5 a,b and Table 1) are comparable to those obtained by Quesnel et al. (2013). The oxygen isotope compositions of magnesites are homogeneous, with $\delta^{18}O$ values in the range of 27.8‰ - 29.5‰. The small variation in $\delta^{18}O$ values does not correlate with any structural or textural characteristics of magnesite. The $\delta^{13}C$ values vary between −15.3‰ and −9.1‰ (Fig. 5b,c and Table 1). The highest $\delta^{13}C$ values correspond to nodular magnesite from soil. The low values between −15.3‰ and −12.1‰

correspond to veins from the Serpentine Sole or from highly serpentinized peridotite (sample GMAR-5).

The Δ_{47} values and clumped isotope temperatures in magnesite are reported in Table 1 and illustrated in Figure 5d. The detailed clumped isotope data are presented in the Electronic Supplement S.1. The clumped isotope temperatures presented here are calculated using the Δ_{47} calibration for calcium carbonate of Kluge et al. (2015), because to date, no Δ_{47} calibration exists for magnesite. The temperatures range between 26-42ºC (Fig. 5d and Table 1) with an average temperature of 30±5ºC for the magnesite veins from the Serpentine Sole and a temperature of 42±2ºC for a nodular soil magnesite.

5.2 Quartz veins and amorphous silica

The oxygen isotope compositions of quartz veins and amorphous silica display a large range of $\delta^{18}O$ values between 21.8‰ and 35.3‰ (Fig. 5a and Table 1). The values higher than 30‰ correspond to translucent or brown opal . Quartz veins from the coarse saprolite level have a total range of $\delta^{18}O$ values between 21.8‰ and 29.0‰, most values being between 24‰ and 28.5‰. There is no systematic difference between quartz and brown micro-crystalline quartz.

6. DISCUSSION

6.1 Conditions of carbonation

6.1.1 Low temperature geochemistry

The oxygen isotope composition of magnesite samples are included in the range ($27.4‰ \leq \delta^{18}O_{Magnesite} \leq 29.7‰$), similar to the results of Quesnel et al. (2013). A first range of temperature of formation of magnesite veins between ~40°C-80°C was estimated by Quesnel et al. (2013) using the oxygen fractionation factor between magnesite and water of Chacko and Deines (2008) and a $\delta^{18}O$ range of fluid composition between -1‰ and -7‰ which correspond to values of rainwater on isolated island at inter-tropical latitude and low elevation (IAEA database: http://www-naweb.iaea.org/napc/ih/IHS_resources_gnip.html). If other oxygen fractionation factors would have been used (see details in Electronic Supplement S.2

and S.3), the calculated temperature range would be lower, the lowest range (~2°C and 40°C) being reached with the fractionation factor of Aharon (1988). Clumped isotope thermometry is particularly useful in such situation when i) several distinct fractionation factors do not converge towards the same range of temperature of mineral formation and ii) uncertainties on the initial fluid composition is particularly large. To calculate the clumped temperature from Δ_{47} values, Falk and Kelemen (2015) used the calibration of Bristow et al. (2011) but in our case, we favor the use of the recent laboratory calibration for calcium carbonate of Kluge et al. (2015) performed in the same laboratory than our study. Actually, for our samples, the clumped isotope temperatures calculated using these two calibrations are similar, taking into account the uncertainties of the measurements. The clumped isotope temperatures obtained using the calibration of Kluge et al. (2015) average around 30°C, and would suggest that the magnesite-water fractionation factors of Aharon (1988; Magnesite 1) and Zheng (1999) are the most consistent with our results.

We use the isotopic equilibrium between amorphous silica and magnesite to test the validity of the calculated clumped temperature of magnesite formation. We were able to obtain the $\delta^{18}O$ of magnesite, $\delta^{18}O$ of amorphous silica and Δ_{47} on magnesite measurements for one sample (GBMS-Si-1, Fig.4g,h and Table 1) where magnesite and amorphous silica are intimately associated and are interpreted as cogenetic. At the serpentine sole level where sample GBMS-Si-1 was collected, pervasive development of amorphous silica linked to magnesite formation by serpentine dissolution is documented (Ulrich et al., 2014). The isotopic fractionation between silica and magnesite ($\Delta^{18}O_{\text{Amorphous silica-Magnesite}}$) measured on this sample is 4.2‰. Actually, there is no published isotopic fractionation factor between these two species. We therefore combine the various oxygen fractionation factors between silica forms and H_2O and magnesite and H_2O available in the literature in order to obtain the corresponding temperature (Electronic supplement S.4). Only three different combinations provide realistic temperatures, around 25°C for two of them and around 40°C for the third. On the same sample GBMS-Si-1, the Δ_{47} measurement allows calculating a temperature of 35±6°C (Table 1), broadly consistent with these temperatures. It thus appears that both methods agree with each other, despite the lack of a specific Δ_{47} calibration for magnesite. More generally, the range of clumped

isotope temperatures between 26±4 and 42±2 calculated for magnesite confirms its low temperature of formation in the Koniambo massif.

6.1.2 Meteoric origin of the fluid

Since clumped isotope thermometry allows estimating the temperatures of formation of carbonate independently of the knowledge of the fluid composition, we can calculate the $\delta^{18}O$ of the fluid from which magnesite formed. The fact that magnesite veins are commonly decimeter thick and abundant on the studied outcrops implies that a large amount of fluid has been involved in their formation. This suggests a high fluid/rock ratio during the fluid circulation through the nappe. The observation that the $\delta^{18}O$ values of magnesite are homogeneous (Fig. 5a) pleads for such conditions. Consequently, we consider that the calculated $\delta^{18}O$ value of the fluid represents its initial composition and not a composition buffered by the host rock during its circulation through the nappe. Given the consistency between temperature estimate using quartz-magnesite equilibrium and clumped isotopes, we use here the oxygen fractionation between magnesite and water from Zheng (1999). The calculated fluids for the 7 magnesite samples have $\delta^{18}O$ values ranging from -3.4‰ to +1.5‰ (Table.1). The 6 negative $\delta^{18}O$ values have an average of -2.5‰ with a minimum at -3.4‰ and a maximum at -0.6‰. They correspond to magnesite veins occurring at the Serpentine Sole. The highest value ($\delta^{18}O$ = +1.5‰) corresponds to a nodular magnesite occurring in a recent soil (DECH1). The oxygen isotope compositions of the fluid are homogeneous and consistent with the present day composition of rainwater on isolated island at inter-tropical latitude and low elevation ranging from -7‰ to -1‰ (AIEA database: http://www-naweb.iaea.org/napc/ih/IHS_resources_gnip.htlm). For the nodular magnesite, the positive oxygen fluid composition is interpreted as evaporation at surface conditions which leaves residual water enriched in ^{18}O. The higher clumped temperature of 42ºC calculated for this sample seems consistent with the slightly higher temperature needed to precipitate magnesite through evaporation of surface waters.

6.1.3 Fractionation in the carbon isotope system

Whereas the $\delta^{18}O$ values of magnesite veins are homogeneous and suggest a single meteoric origin of the fluid from which they formed, the large spread of $\delta^{13}C$ values implies several sources of carbon and/or specific fractionation effect in the carbon isotope system. The highest $\delta^{13}C$ values, around -9‰, could result from various sources of carbon. An atmospheric CO_2 contribution could, at least in part, explain these high values. A biogenic soil source could also be dominant. Indeed, this would be consistent with the fact that magnesite with such $\delta^{13}C$ values are nodular magnesites from soil and are probably formed in-situ by evaporation as previously explained for sample "DECH1". Most of the magnesite samples from the Serpentine Sole have lower $\delta^{13}C$ values between -15.3‰ and -12.1‰. An organic carbon contribution from surface soil or from decarboxylation of deep seated organic matter-rich sediments could explain such low values.

Independently, several resurgences of hyperalkaline fluid with pH up to 11 related to present day serpeninization (Barnes et al., 1978, Monin et al., 2014) occur in New Caledonia (Launay and Fontes, 1985). Among the processes that could explain low values of $\delta^{13}C$, kinetic isotopic fractionation of C isotopes is known during hydroxylation of dissolved CO_2 when carbonate forms by diffusive uptake of dissolved CO_2 (Dietzel et al., 1992). Such process has been proposed to explain the extreme depletion of ^{13}C measured in various carbonate occurrences, without important effect on the oxygen isotope compositions, as calcite travertine deposit in Oman (Clark et al., 1992), sediments cemented by calcite from central Jordan (Fourcade et al., 2007) and also for magnesite deposits in Australia (Oskierski et al., 2013).

Recently, Hill et al. (2014) and Watkins and Hunt (2015) showed that kinetic fractionation in alkaline to hyperalkaline environment have minor effect on the $\Delta 47$ composition of carbonate. This can lead to underestimate the clumped isotope temperature of mineral growth by a few °C. Even if such effect would have existed during magnesite formation, this thus would not change the conclusion that magnesite formed at low temperature, around 30°C.

6.2 Conditions of quartz veins and amorphous silica formation

At the island scale, the $\delta^{18}O$ values of quartz veins and amorphous silica spread over

a range of ~15‰. The fact that all quartz veins and amorphous silica occur in the peridotite and commonly in deformation zones (at the serpentine sole or as fractures or faults infillings) suggest that they are probably genetically linked to a unique fluid reservoir. We argued in section 6.1.2 that an amorphous silica sample ($\delta^{18}O$ = 33‰) formed in isotopic equilibrium with magnesite (sample GBMS-Si-1) from a meteoric water at low temperature. By inference, we consider that all amorphous silica occurrences formed from a meteoric fluid. For the quartz veins, their structural position (i.e. at the base of the laterite profile, in the saprolite) and their association with garnierite strongly suggest that the fluid from which they formed also have a meteoric origin. Considering the low variability of paleo-latitude of New Caledonia during the 30 last million years (Paleomap project: http://gcmd.nasa.gov/records/PALEOMAP-Serf.html) and by consequence the limited variation of the isotopic composition of rainwater during that period, variations in temperature are the most likely factor at the origin of the large spread in $\delta^{18}O$ values recorded by silica species. Given that quartz veins are commonly decimeter thick and abundant in the coarse saprolite level it is likely that the system worked under conditions of large fluid/rock ratios, in which case fluids keep their initial isotopic compositions during interaction with rocks. By consequence, the $\delta^{18}O$ of silica materials directly reflect the temperature of formation, as the $\delta^{18}O$ of the fluid is considered as constant. As no oxygen isotope compositions of present-day rainwaters in New Caledonia are available, we use the mean value of the $\delta^{18}O$ values calculated for the meteoric fluid from which magnesite veins formed (mean $\delta^{18}O_{meteoric\text{-}fluid}$ = -2.5‰, see Table.1) to calculate the temperatures of formation of amorphous silica and quartz veins. The use of various oxygen fractionation factors between silica and H_2O (Electronic Supplement S.5) provide similar range of temperature; only the fractionation factor of Bandriss et al. (1998) was unable to provide a temperature consistent with the oxygen isotopic equilibrium between quartz and magnesite for sample GBMS-Si-1 (See section 6.1.1 and Electronic Supplement S.4).

The $\delta^{18}O$ values of amorphous silica samples range between 29.7‰ and 35.3‰, which correspond to temperatures between ~15°C and ~40°C.The quartz veins occurring in the coarse saprolite level have $\delta^{18}O$ values between 21.8‰ and 29.0‰, which correspond to temperature between ~40°C and ~95°C, with most samples recording temperatures between ~40°C and ~80°C.

To summarize, the main information obtained from the isotope systematics on quartz veins from the saprolitic level is that they formed under conditions of low-temperature hydrothermalism rather than at surface temperatures.

6.3 Heat sources for quartz veins formation

Magnesite and amorphous silica have ranges of oxygen composition narrower than that of quartz veins (Fig. 5a, c) which suggests more constant temperatures of formation. The clumped isotope temperatures for magnesite formation are between 26±4°C and 42±2°C, which is consistent with the range of temperature estimated for amorphous silica formation between ~15°C and ~40°C. Even if all amorphous silica are not intimately related to magnesite (typically brown opal silica is not), the fact remains that both their similar temperature of formation and their narrow ranges of $\delta^{18}O$ values suggest that they are genetically linked to the same low temperature fluid. Following Quesnel et al. (2013), we can thus propose that magnesite and amorphous silica occurring at different levels of the nappe record the fluid pathway through the nappe where rapid downward circulation was enhanced by active tectonics.

For quartz veins from the coarse saprolite level the large range of temperature between ~40°C and ~95°C indicates variable conditions and distinctly higher temperatures of formation. The range of temperature estimated for the quartz veins from the coarse saprolite level appears particularly high given their structural position. A first possibility is to invoke upward movements of hot fluids coming from depth. Even if it is difficult to estimate the past thickness of the nappe at the time of fluid circulation, the present-day topographic constraints allow estimating a minimum thickness. The mean elevation in the island scale is ~640m as reported by Chevillotte et al. (2006) and the Mont Panié, located on the northern part of the East coast, culminates at 1628m. Considering a surface temperature of ~25°C, a past thickness of the nappe between ~500 and ~2000m and a paleo-gradient of temperature in the peridotite nappe of 20°C.km^{-1}, temperatures of ~35-75°C may have been reached at the base of the nappe. Rapid upward migration of fluids equilibrated at these temperatures might explain the temperatures recorded by the quartz veins. Occurrences of hydraulic breccia where quartz cements serpentine and garnierite clasts in the coarse saprolite level (Myagkiy et al., 2015) are consistent with this idea.

The question of mechanism of precipitation of quartz in the saprolitic structural level remains. The first possibility consists in the precipitation of quartz lead by a change of pH condition. Indeed quartz solubility is function of pH increasing rapidly from pH>9. The pH measured in New Caledonian resurgences of water at the base of the nappe are basic with pH up to 11 (Monin et al., 2014) whereas pH in coarse saprolite level is around ~8 (Trescases, 1975). This abrupt decrease of pH at the saprolitic interface could explain quartz precipitation. Moreover, an additional mixing with *per descensum* meteoric water with pH ~7 (Trescases, 1975) and at surface temperature is also possible and could lead to quartz precipitation.

Nevertheless, unlike the conditions of syn-tectonic magnesite formation, no clear evidence of syn-tectonic quartz veins formation is recorded and precludes associating the fluid overpressure to tectonic activity. Consequently, even if the upward fluid circulation linked to fluid overpressure may be in agreement with our data, it remains difficult to identify the cause of such large-scale upward migration of fluid.

An alternative hypothesis to explain the ~40-95°C temperature range of formation of quartz veins at the coarse saprolite level is to invoke exothermic reactions of serpentinization. Indeed, such reactions are known to produce heat (Fyfe, 1974) and may explain elevated temperature of fluid in ultramafic-hosted hydrothermal systems (Kelley et al., 2001, Lowell and Rona, 2002, Schroeder et al., 2002). Even if serpentinization reactions can explain only a part of the heat contribution for high temperature hydrothermal systems, they could be sufficient for low temperature hydrothermal system like Lost City type (Mével, 2003). In New Caledonia, several present-day resurgences of low-temperature (reaching 37°C) and hyperalkaline fluid with pH up to 11 are interpreted as evidence of present-day serpentinization (Barnes et al., 1978, Monin et al., 2014). A recent study (Guillou-Frottier et al., 2015) proposes that such reactions could occur in the coarse saprolite during the weathering of the peridotite. These authors argue that serpentinization reactions should trigger convective fluid circulation by i) increasing of temperature by several tens of degrees and ii) increasing of permeability and porosity by fracturation induced by volume expansion (Kelemen and Hirth, 2012). This model could explain the relatively high temperatures identified for the quartz veins formation and the local occurrences of hydraulic breccia where quartz cements serpentine and garnierite (Myagkiy et al., 2015). Our observation and isotopic data are consistent with this model.

7. CONCLUSION

On the basis of stable oxygen isotope data and clumped isotope analyses, we argue that carbonation at the base of the nappe and silicification at the saprolite level of the New Caledonia Peridotite Nappe occurred under different temperature conditions. First, stable isotopes and clumped isotope analyses of magnesite and opal display a narrow range of $\delta^{18}O$ values attesting for formation under homogeneous conditions, at temperature of ~25 to 40°C for magnesite and between ~15°C and ~40°C for amorphous silica. The oxygen isotope compositions estimated for the fluid at the origin of magnesite and amorphous silica are consistent with meteoric water compositions. Second, the $\delta^{18}O$ values of quartz veins from the coarse saprolite level display a large range, which is indicative of formation between ~40°C and ~95°C, typical temperatures of low temperature hydrothermalism.

These results lead to question the classical *per descensum* model of Ni-laterites ore deposit where silica, magnesium and nickel leached during supergene alteration of peridotite are exported by downward fluid circulation along fractures cutting through the nappe. Indeed, our results tends to show that carbonation of the Serpentine Sole and quartz veins formation at the coarse saprolite level are the results of two distinct fluid circulation systems. If the low-temperatures conditions of magnesite formation, specified here using clumped isotope thermometry, are consistent with the tectonically enhanced downward meteoric water circulation model previously proposed in Quesnel et al. (2013), higher temperatures of quartz veins formation would imply that a refinement of the classical *per descensum* model is needed. Thermal equilibration of the fluid along a normal geothermic gradient through the nappe or influence of exothermic reactions of serpentinization could explain such temperatures. Regardless of the exact explanation, it means that nickel lateritic mineralization, with which the quartz veins studied here are associated, developed under conditions of low-temperature hydrothermalism. This inference may be of importance with regards to the properties of migration of nickel during mineralization.

ACKNOWLEDGEMENTS

This study constitutes a part of B. Quesnel PhD which is supported financially and technically by Koniambo S.A. This study has benefited from equipment purchased by the Qatar Carbonate and Carbonate Storage Research Center sponsored by Qatar Petroleum, Shell, and the Qatar Science and Technology Park. PB and MC thank Emmanuel Fritsch for the geological tour he organized in the CNRT framework. Mineralogical investigations carried out at Nancy were done within the framework of Labex Ressources 21 (supported by the French National Research Agency through the national program "Investissements d'avenir", reference ANR-10-LABX-21–LABEX RESSOURCES 21).

FIGURES

Figure 1- Simplified geological map of New Caledonia. Ultramafic rocks are from Maurizot and Vendé-Leclerc (2009) and laterites are adapted from Paris (1981).

Figure 2- Geological map of the Koniambo massif adapted from Maurizot (2002). Numbers indicate sampling location and are reported in Table 1 for all samples coming from the Koniambo massif.

Figure 3- Field observations of magnesite occurrences. A-C: Field views of magnesite veins occurring at the serpentine sole. A: field view illustrating relationship between magnesite veins and shear zone. The thickest vein occurs in the main shear band whereas the thinnest occur in C'-type shear bands. B,C: field view illustrating the fibrous texture of magnesite veins. D: field view of nodular magnesite occurring in a soil. Sample numbers are indicated and are reported in Table 1.

Figure 4- A,C,D: field view of quartz veins occurring in the coarse saprolite level of Koniambo massif. B,F: sawed sections through two hand specimen showing complex textural relationships between B: brown micro-crystalline quartz and yellow and white quartz and F: brown micro-crystalline quartz, translucent quartz and clasts of serpentine (in green). G,E: field view of amorphous silica. G: translucent opal associated with magnesite at the Serpentine Sole. H: hand sample GBMS-SI-1 where

magnesite and amorphous silica are cogenetic. E: brown opal occurring as late coating on blocks of the coarse saprolite. Sample locations are indicated by a white star and are reported in Table 1.

Figure 5- The light grey color represents samples from the Koniambo massif, those in dark grey are from elsewhere on the island. All the sample locations are reported in the figures. 1,2 and in Table 1. The isotopic values are given versus VSMOW (Vienna Standard Mean Ocean Water) for $\delta^{18}O$ and versus VPDB (Vienna PeeDee Belemnite) for $\delta^{13}C$. A: histogram of $\delta^{18}O$ values of magnesite samples (veins and nodules) B: $\delta^{13}C$ versus $\delta^{18}O$ diagram of magnesite samples. C: histogram of $\delta^{18}O$ values of quartz veins amorphous silica. D: diagram showing the temperature calculated from Δ_{47} analyses using the calibration of Kluge et al. (2015) as a function of the $\delta^{18}O$ values of 7 magnesite samples.

Table 1- Δ_{47}, $\delta^{18}O$ and $\delta^{13}C$ values of magnesite samples and $\delta^{18}O$ values of silica samples. "n" indicates the number of replicate samples analyzed by clumped isotope thermometry. T (Δ_{47}) uncertainty is estimated on the basis of the 1SE analytical uncertainty in measured Δ_{47} propagated through the Kluge et al. (2015) equation. The $\delta^{18}O$ of the fluid from which magnesite formed is calculated using the clumped isotope temperature and the oxygen fractionation factor between magnesite and H_2O of Zheng (1999).

REFERENCES

Affek, H.P., Eiler, J.M. (2006) Abundance of mass 47 CO_2 in urban air, car exhaust, and human breath. *Geochim. Cosmochim. Acta* **70**, 1–12.

Aharon, P. (1988) A stable-isotope study of magnesites from the rum jungle uranium field, Australia : implications for the origin of strata-bound massive magnesites. *Chemical Geology* **69**, 127-145

Aye, F., Bonnemaison, M., Jacob, M. (1986) Etude gîtologique et géochimique des indices et anomalies en Sb, W, As, Au de la côte Est de la Nouvelle-Calédonie-

programme CORDET-Rapport final du projet A4 (1983-84). Bureau des Recherches Géologiques et Minières report 85 NCL 079 GMX.

Bandriss, M.E., O'Neil, J.R., Edlund, M.B., Stoermer, E.F. (1998) Oxygen isotope fractionation between diatomaceous silica and water. *Geochimica et Cosmochimica Acta* **62**, 1119-1125.

Barnes, I., O'Neil, J. R., and Trescases, J. J. (1978) Present day serpentinization in New Caledonia, Oman and Yugoslavia. *Geochimica et Cosmochimica Acta* **42**, 144–145.

Barnes, I., O'Neil, J.R., Rapp, J.B., White, D.E. (1973) Silica-carbonate alteration of serpentine: wall rock alteration in Mercury deposits of the California Coast Ranges. *Economic Geology* **68**, 388-398.

Beinlich, A., Plümper, O., Hövelmann, J., Austrheim, H., Jamtveit, B. (2012) Massive serpentinite carbonation at Linnajavri, N-Norway. *Terra Nova* **24**, 446-455.

Bristow T. F., Bonifacie M., Derkowski A., Eiler J. M. and Grotzinger J. P. (2011) A hydrothermal origin for isotopically anomalous cap dolostone cements from south China. *Nature* **474**, 68–71. http://dx.doi.org/10.1038/nature10096.

Brindley, G.W., Hang, P.T. (1973) The nature of garnierites—I—Structures, chemical compositions and color characteristics. *Clays and Clay Minerals* **21**,27-40.

Butt, C.R., Cluzel, D. (2013) Nickel laterite ore deposits: weathered serpentinites. *Elements* **9**, 123-128.

Cathelineau, M., Caumon, M-C., Massei, F., Brie, D., Harlaux, M. (2015a) Raman spectra of Ni-Mg kerolite: effect of Ni-Mg substitution on O-H stretching vibrations. *Journal of Raman Spectroscopy,* Proceedings GEORaman 2014 (11th), St Louis (USA)

Cathelineau, M., Quesnel, B., Gautier, P., Boulvais, P., Couteau, C., Drouillet, M. (2015b) Nickel dispersion and enrichment at the bottom of the regolith : formation of pimelite target-like ores in rock block joints (Koniambo Ni Deposit, New Caledonia). *Mineralium Deposita,* 1-12.

Chacko T., Deines P. (2008) Theoretical calculation of oxygen isotope fractionation factors in carbonate systems. *Geochim. Cosmochim. Acta* **72**, 3642–3660 doi:10.1016/j .gca.2008.06.001.

Chevillotte, V., Chardon, D., Beauvais, A., Maurizot, P., Colin, F. (2006) Long-term tropical morphogenesis of New Caledonia (Southwest Pacific): Importance of positive epeirogeny and climate change. *Geomorphology* **81**, 361-375.

Clark, I.D., Fontes, J.C., Fritz, P. (1992) Stable isotope disequilibria in travertine from high pH waters: laboratory investigations and field observations from Oman. *Geochim. Cosmochim. Acta* **56**, 2041-2050.

Clayton, R., Mayeda, K. (1963) The use of bromine pentafluoride in the extraction of oxygen from oxides and silicates for isotopic analyses. *Geochim. Cosmochim. Acta* **27**, 43-52.

Cluzel, D., Maurizot, P., Collot, J., Sevin, B., (2012) An outline of the geology of New Caledonia; from Permian-Mesozoic Southeast Gondwanaland active margin to Cenozoic obduction and supergene evolution. *Episodes* **35**, 72–86.

Cluzel, D., Vigier, B. (2008) Syntectonic Mobility of Supergene Nickel Ores of New Caledonia (Southwest Pacific). Evidence from Garnierite Veins and Faulted Regolith. *Resource Geology* **58**, 161–170. doi:10.1111/j.1751-3928.2008.00053.x

Craig, H., Boato, G. (1955) Isotopes. *Annual review of physical chemistry* **6**, 403-432.

Das Sharma, S., Patil, D.J., and Gopalan, K. (2002) Temperature dependence of

oxygen isotope fractionation of CO_2 from magnesite–phosphoric acid reaction. *Geochim. Cosmochim. Acta* **66**, 589–593. doi:10.1016/S0016-7037 (01)00833-X.

Dennis K. J., Affek H. P., Passey B. H., Schrag D. P. and Eiler J. M. (2011) Defining an absolute reference frame for 'clumped' isotope studies of CO2. *Geochim. Cosmochim. Acta* **75**, 7117– 7131. http://dx.doi.org/10.1016/j.gca.2011.09.025.

Dennis, K., Schrag, D. (2010) Clumped isotope thermometry of carbonatites as an indicator of diagenetic alteration. *Geochim. Cosmochim. Acta* **74**, 4110-4122.

Dietzel, M., Usdowski, E., Hoefs, J. (1992) Chemical and $^{13}C/^{12}C$- and $^{12}O/^{16}O$-isotope evolution of alkaline drainage waters and the precipitation of calcite. *Applied Geochemistry* **7**, 177-184.

Dublet, G., Juillot, F., Morin, G., Fritsch, E., Fandeur, D., Brown Jr., G.E. (2015) Goethite aging explains Ni depletion in upper units of ultramafic lateritic ores from New Caledonia. *Geochim. Cosmochim. Acta* **160**, 1-15. http://dx.doi.org/10.1016/ j.gca.2015.03.015.

Ducloux, J., Boukili, H., Decarreau, A., Petit, S., Perruchot, A., Pradel, P. (1993) Un gîte hydrothermal de garnierites: l'exemple de Bou Azzer, Maroc. *Eur. J. Mineral.* **5**,1205-1215.

Eiler J.M. (2007) **"**Clumped-isotope" geochemistry—The study of naturally-occurring, multiply-substituted isotopologues. *Earth and Planetary Science Letters* **262**, 309–327. doi: 10.1016/j.epsl.2007.08.020.

Eiler, J.M., Schauble, E. (2004) $^{18}O^{13}C^{16}O$ in Earth's atmosphere. *Geochim. Cosmochim. Acta* **68 (23)**, 4767–4777. Doi:10.1016/j.gca.2004.05.035

Emiliani, C. (1966) Isotopic paleotemperatures. Science **154**, 851-857

Epstein, S., Buchsbaum, R., Lowenstam, H.A., Urey, H.C. (1953) Revised carbonate-

water isotopic temperature scale. *Bulletin of the geological society of America* **64**, 1315-1326.

Fallick, A.E., Ilich, M., and Russell, M.J. (1991) A stable isotope study of the magnesite deposits associated with the Alpine-type ultramafic rocks of Yugoslavia. *Economic Geology and the Bulletin of the Society of Economic Geologists* **86**, 847–861. doi:10.2113/gsecongeo.86.4.847.

Falk, E.S., Kelemen, P.B. (2015) Geochemistry and petrology of listvenite in the Samail ophiolite, Sultanate of Oman: complete carbonation of peridotite during ophiolite emplacement. *Geochim. Cosmochim. Acta* **160**, 70-90. http://dx.doi.org/10.1016/j.gca.2015.03.014

Faust, G.T. (1966) The hydrous nickel-magnesium silicates—the garnierite group. *The American mineralogist* **51**, 279-298.

Fourcade S., Trotignon L., Boulvais P., Techer I., Elie M., Vandamme D., Salameh E., Khoury H. (2007) Cementation of kerogene-rich marls by alkaline fluids released during weathering of thermally metamorphosed marly sediments. Part I: Isotopic (C, O) study of the Khushaym Matruk natural analogue (central Jordan). *Applied Geochemistry* **22**, 1293-1310.

Freyssinet P., Butt C.R.M., Morris R.C., Piantone P. (2005) Ore-forming processes related to lateritic weathering. In: Hedenquist JW, Thomson JFH, Goldfarb RJ, Richards JP (eds), Economic Geology 100th Anniversary Volume. Economic Geology Publishing Company, New Haven, Connecticut, pp 681-722$

Fritsch, E.M., Juillot, F.A., Dublet, G.A., Fonteneau, L., Fandeur, D., Martin, E., Caner, L., Auzende, A-L., Grauby, O., Beaufort, D. (2015) An alternative model for the formation of hydrous Mg / Ni layer silicates (“ deweylite ”/“ garnierite ”) in faulted peridotites of New Caledonia : I . Texture and mineralogy of a paragenetic

succession of silicate infillings. *European Journal of Mineralogy*, in press, doi: 10.1127/ejm/2015/0027-2503

Fyfe, W.S. (1974) Heats of chemical reactions and submarine heat production. *Geophysical journal of the Royal Astronomical Society***37**, 213-215.

Gartzos, E. (2004) Comparative stable isotopes study of the magnesite deposits of Greece. *Bulletin of the Geological Society of Greece* **36**, 196–203.

Glasser E. (1904) Rapport à M le Ministre des Colonies sur les richesses minérales de la Nouvelle- Calédonie. Paris, Annales des Mines, 560 p.

Ghosh P., Adkins J., Affek H., Balta B., Guo W., Schauble E. A., Schrag D. and Eiler J. M. (2006) ^{13}C–^{18}O bonds in carbonate minerals: a new kind of paleothermometer. *Geochim. Cosmochim. Acta* **70**, 1439–1456.

Golyshev, S.I., Padalko, N.L., Pechenkin, S.A. (1981) Fractionation of stable oxygen and carbon isotopes in carbonate systems. *Geokhimiya* **10**, 1427-1441 (in Russia)

Guillou-Frottier, L., Beauvais, A., Bailly, L., Wyns, R., Augé, T., Audion, A-S. (2015) Transient hydrothermal corrugations within mineralized ultramafic laterites. In: Proceedings of the 1"th Biennal SGA (Society for Geology Applied to Mineral Deposits) meeting, 24-27 August 2015, Nancy, France, vol.3, 1169-1172.

Guo, W. F., Mosenfelder, J. L., Goddard, W. A. and Eiler, J. M. (2009) Isotopic fractionations associated with phosphoric acid digestion of carbonate minerals: insights from first-principles theoretical modeling and clumped isotope measurements. *Geochim. Cosmochim. Acta* **73**, 7203–7225.

Hill, P.S., Tripati, A.K., Schauble, E.A. (2014) Theoretical constraints on the effects of pH , salinity , and temperature on clumped isotope signatures of dissolved inorganic carbon species and precipitating carbonate minerals. *Geochim Cosmochim Acta* **125**, 610–652.

Huntington K. W., Eiler J. M., Affek H. P., Guo W., Bonifacie M., Yeung L. Y., Thiagarajan N., Passey B., Tripati A., Daëron M., and Came R. (2009) Methods and limitations of 'clumped' CO_2 isotope (Δ_{47}) analysis by gas-source isotope ratio mass spectrometry. *J. Mass. Spectrom.* **44**, 1318–1329.

Jacob, M. (1985) Etude géologique, minéralogique et géochimique des anomalies en As, Sb, Au et W et indices minéralisés liés aux fractures regionals de la côte sud-est de la Nouvelle-Calédonie. Ph.D thesis, University Paul Sabatier, Toulouse, n°3138, 155p.

Jedrysek, M.O., and Halas, S. (1990) The origin of magnesite deposits from the Polish Foresudetic Block ophiolites: Preliminary $\delta^{13}C$ and $\delta^{18}O$ investigations. *Terra Nova* **2**, 154–159. doi:10.1111/j.1365-3121.1990.tb00057.x.

Jurkovic, I., Palinkas, L.A., Garasic, V., and Strmic Palinkas, S. (2012) Genesis of vein-stockwork cryptocrystalline magnesite from the Dinaride ophiolites. *Ofioliti* **37**, 13–26.

Kelemen, P.B., Hirth, G. (2012) Reaction-driven cracking during retrograde metamorphism: Olivine hydratation and carbonation. *Earth and Planetary Science Letters* **345-348**, 81-89.

Kelemen, P.B., Matter, J. (2008) In situ carbonation of peridotite for CO_2 storage. *PNAS* **105(45)**, 17295-17300

Kelemen, P., Matter, J., Streit, E.E., Rudge, J.F., Curry, W.B., Blusztajn, J. (2011) Rates and mechanisms of mineral carbonation in peridotite: natural processes and recipes for enhanced, in situ CO2 capture and storage. *Annual Review of Earth and Planetary Sciences* **39**, 545–576. doi:10.1146/annurev-earth-092010-152509

Kelley, D.S., Karson, J.A., Blackman, D.K., Früh-Green, G.L., Butterfield, D.A., Lilley, M.D., Olson, E.J., Schrenk, M.O., Roe, K.K., Lebon, G.T., Rivissigno, P.,

AT3-60 shipboard party (2001) An off-axis hydrothermal vent field near the Mid-Atlantic Ridge at 30°N. *Nature* **412,** 145-149.

Kita, I., Taguchi, S., Matsubaya, O. (1985) Oxygen isotope fractionation between amorphous silica and water at 34-93°C. *Nature* **314**, 83-84.

Kluge, T., John, C.M., Jourdan, A.L., Davis, S., Crawshaw, J. (2015) Laboratory calibration of the calcium carbonate clumped isotope thermometer in the 25-250˚C temperature range. *Geochim. Cosmochim. Acta* **157**, 213-227. doi:10.1016/j.gca.2015.02.028

Launay, J., Fontes, J.C. (1985) Les sources thermales de Prony (Nouvelle-Calédonie) et leurs précipités chimiques. Exemple de formation de brucite primaire. *Géologie de la France* **1**, 83-100.

Latham, M. (1977) On geomorphology of northern and western New Caledonian ultramafic massifs. International symposium on geodynamics in south-west Pacific, Nouméa, Technip Paris éd, 235-244.

Latham, M. (1986) Altération et pédogenèse sur roches ultrabasiques en Nouvelle-Calédonie: Editions de l'ORSTOM (Office de la Recherche Scientifique et Technique Outre-Mer), Collection Etudes et Theses.

Lowell, R.P., Rona, P.A. (2002) Seafloor hydrothermal systems driven by the serpentinization of peridotite. *Geophysical research letters* **29 (11).**

McCrea, J. M. (1950) On the isotopic chemistry of carbonates and a paleotemperature scale. Journal of Chemical Physics **18**, 849-857.

Maurizot, P., Lafoy, Y., and Poupée, M. (2002) Cartographie des formations superficielles et des aléas mouvements de terrain en Nouvelle-Calédonie, Zone du Koniambo: Bureau de Recherches Géologiques et Minières Public Report RP51624-FR, 45 p.

Maurizot, P., Vendé-Leclerc, M. (2009) New Caledonia geological map, scale 1/500000, DIMENC-SGNC, BRGM. Explanatory note by Maurizot, P. and Collo, J.

Meckler, A.N., Ziegler, M., Millan, M.I., Breitenbach, S.F.M., Bernasconi, S.M. (2014) Long-term performance of the Kiel carbonate device with a new correction scheme for clumped isotope measurements. *Rapid Commun. Mass Spectrom.* **28 (15),** 1705-1715.

Mével, C. (2003) Serpentinization of abyssal peridotites at mid-ocean ridges. *C.R. Geosciences* **335**, 825-852.

Monin, C., Chavagnac, V., Boulart, C., Ménez, B., Gérard, M., Gérard, E., Quéméneur, M., Erauso, G., Postec, A., Guentas-Dombrowski, L., Payri, C., Pelletier, B. (2014) The low temperature hyperalkaline hydrothermal system of the Prony bay (New Caledonia). *Biogeosciences Dicuss.* **11**, 6221-6267.

Myagkiy, A., Cathelineau, M., Golfier, F., Truche, L., Quesnel, B., Drouillet, M. (2015) Defining mechanisms of brecciation in Ni-Silicate bearing fractures (Koniambo, New Caledonia). In: Proceedings of the 1"th Biennal SGA (Society for Geology Applied to Mineral Deposits) meeting, 24-27 August 2015, Nancy, France, vol.3, 1181-1194.

Oelkers, E.H., Sigurdur, R.G., Matter, J. (2008) Mineral carbonation of CO_2. *Elements* **4**, 333-337.

Oskierski, H.C., Bailey, J.G., Kennedy, E.M., Jacobsen, G., Ashley, P.M., and Dlugogoski, B.Z. (2013) Formation of weathering-derived magnesite deposits in the New England Orogen, New South Wales, Australia: Implications from mineralogy, geochemistry and genesis of the Attunga magnesite deposit. *Mineralium Deposita* **48**, 525–541. doi:10.1007/s00126-012-0440-5.

Paquette, J.L., and Cluzel, D. (2007) U-Pb zircon dating of post-obduction volcanic-arc granitoids and a granulite-facies xenolith from New Caledonia: Inference on Southwest Pacific geodynamic models. *International Journal of Earth Sciences* **96**, 613–622. doi:10.1007/s00531-006-0127-1.

Paris, J.P. (1981) Géologie de la Nouvelle-Calédonie: un essai de synthèse. *Mémoire du BRGM (Bureau de Recherches Géologiques et Minières)* **113**.

Quesnel B., Gautier P., Boulvais P., Cathelineau M., Maurizot P., Cluzel D., Ulrich M., Guillot S., Lesimple S., Couteau C. (2013) Syn-tectonic, meteoric water-derived carbonation of the New Caledonia peridotite nappe. *Geology* **41**, 1063–1066. doi:10.1130/G34531.1

Quesnel, B., Gautier, P., Cathelineau, M., Boulvais, P., Couteau, C., Drouillet, M. (2016) The internal deformation of the Peridotite Nappe of New Caledonia : a structural study of serpentine-bearing faults and shear zones in the Koniambo Massif. *Journal of Structural Geology* **85**, 51-67.

Sabouraud, C., Trichet, J. (1978) Confirmation, par l'étude des inclusions intracristallines, de l'origine superficielle de quartz pyramides. *Geoderma* **20**, 191-199.

Sevin, B., Ricordel-Prognon, C., Quesnel, F., Cluzel, D., Lesimple, S., and Maurizot, P. (2012) First palaeomagnetic dating of ferricrete in New Caledonia: New insight on the morphogenesis and palaeoweathering of 'Grande Terre'. *Terra Nova* **24**, 77–85, doi:10.1111/j.1365-3121 .2011.01041.x.

Schauble, E.A., Ghosh, P., Eiler, J.M. (2006) Preferential formation of 13C-18O bonds in carbonate minerals, estimated using first-principle lattice dynamics. *Geochimica et Cosmochimica Acta* **70**, 2510-2529.

Schroeder, T., John, B., Frost, R.B. (2002) Geologic implications of seawater circulation through peridotite exposed at slow-spreading mid-ocean ridges. *Geology* **30**, 367-370.

Sharp, Z.D., Kirschner, D.L. (1994) Quartz-calcite oxygen isotope thermometry: a calibration based on natural isotopic variations. *Geochim. Cosmochim. Acta* **58(21)**, 4491-4501.

Streit, E., Kelemen, P., Eiler, J. (2012) Coexisting serpentine and quartz from carbonate-bearing serpentinized peridotite in the Samail Ophiolite, Oman. *Contrib. Mineral. Petrol.* **164(5)**, 821-837. doi:10.1007/s00410-012-0775-z

Trescases, J.J. (1975) L'évolution géochimique super- gène des roches ultrabasiques en zone tropicale: Formation des gisements nickélifères de Nouvelle-Calédonie. Mémoires ORSTOM (Office de la Recherche Scientifique et Technique Outre-Mer) 78, 259 p.

Ulrich, M., Muñoz, M., Guillot, S., Cathelineau, M., Picard, C., Quesnel, B., Boulvais, P., Couteau, C. (2014) Dissolution-precipitation processes governing the carbonation and silicification of the serpentine sole of the New Caledonia ophiolite. *Contrib. Mineral. Petrol.* **167**, 952.

Urey, H.C. (1947) The thermodynamic properties of isotopic substances. *Journal of the Chemical Society,* 562-581.

Villanova-de-Benavent C., Proenza J.A., Galí S., García-Casco A., Tauler E., Lewis J.F., Longo F. (2014) Garnierites and garnierites: textures, mineralogy and geochemistry of garnierites in the Falcondo Ni-laterite deposit, Dominican Republic. *Ore Geol Rev* **58**, 91–109.

Wacker U., Fiebig J., Schoene B. R. (2013) Clumped isotope analysis of carbonates: comparison of two different acid digestion techniques. *Rapid Commun. Mass Spectrom.* **27**, 1631-1642.

Watkins, J.M., Hunt, J.D. (2015) A process-based model for non-equilibrium clumped isotope effects in carbonates. *Earth Planet Sci Lett* **432**, 152–165

Zheng, Y.-F. (1993) Calculation of oxygen isotope fractionation in anhydrous silicate minerals. *Geochim. Cosmochim. Acta* **57**, 1079-1091.

Zheng, Y.F. (1999) Oxygen isotope fractionation in carbonate and sulfate minerals. *Geochemical Journal* **33**, 109-126.

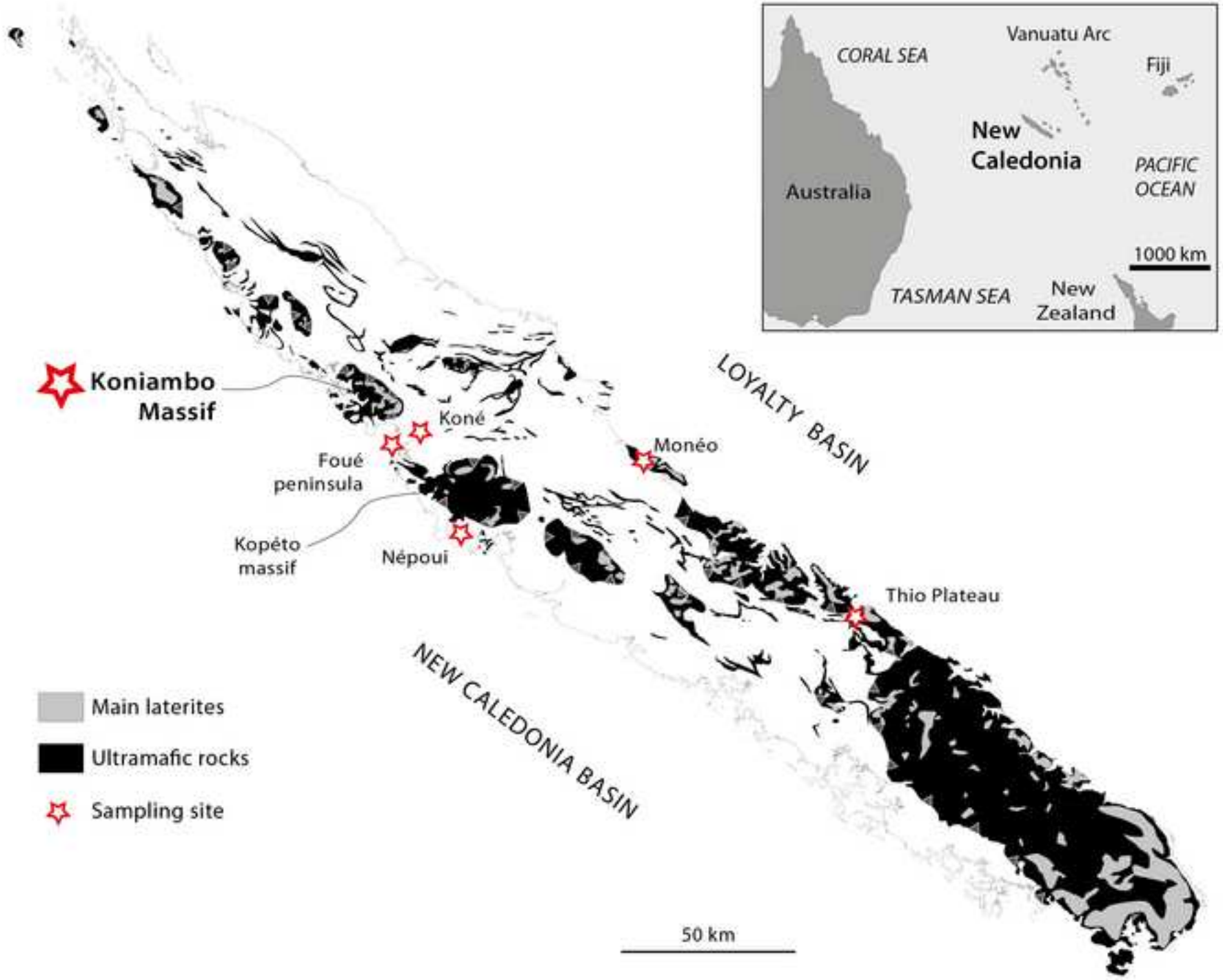

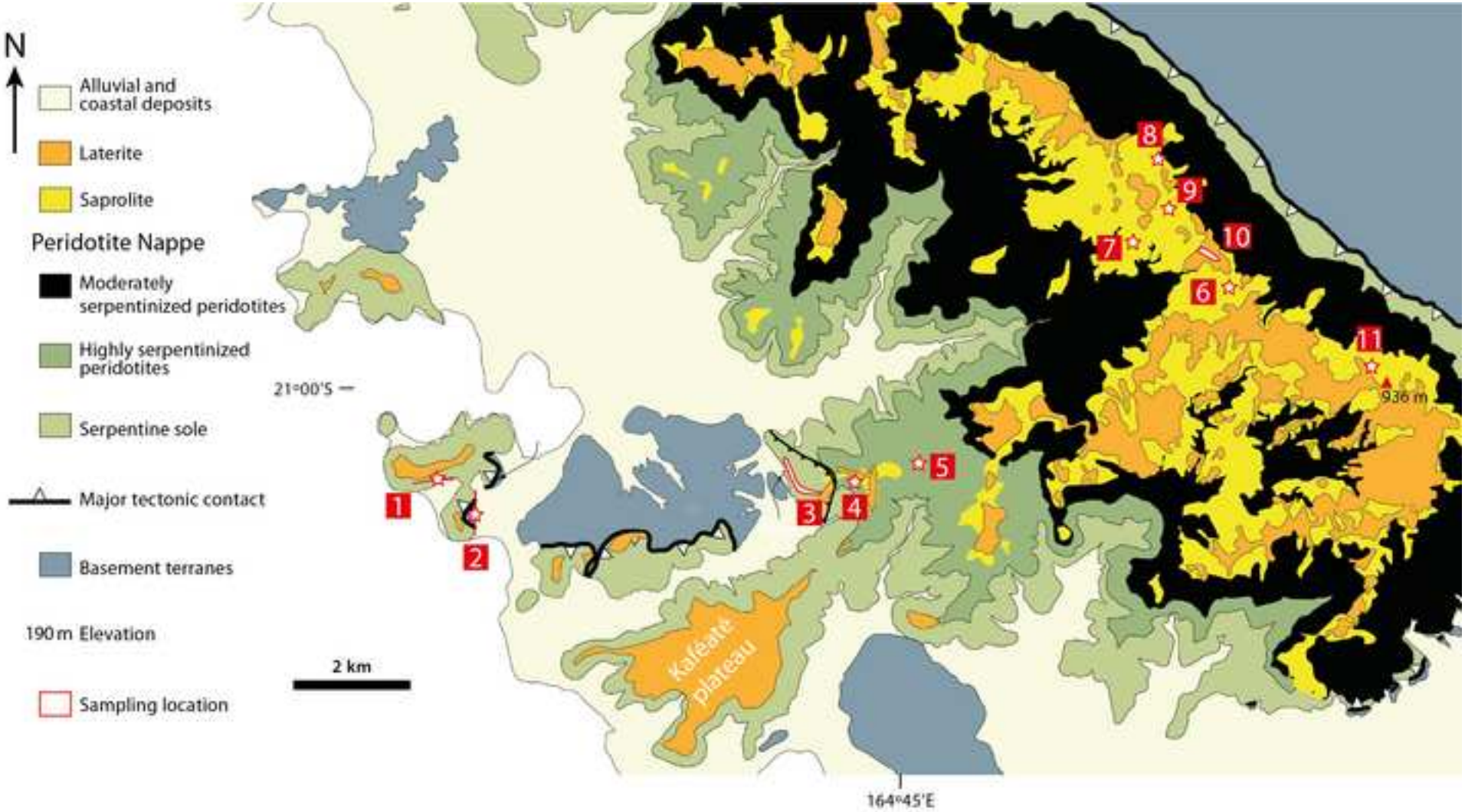

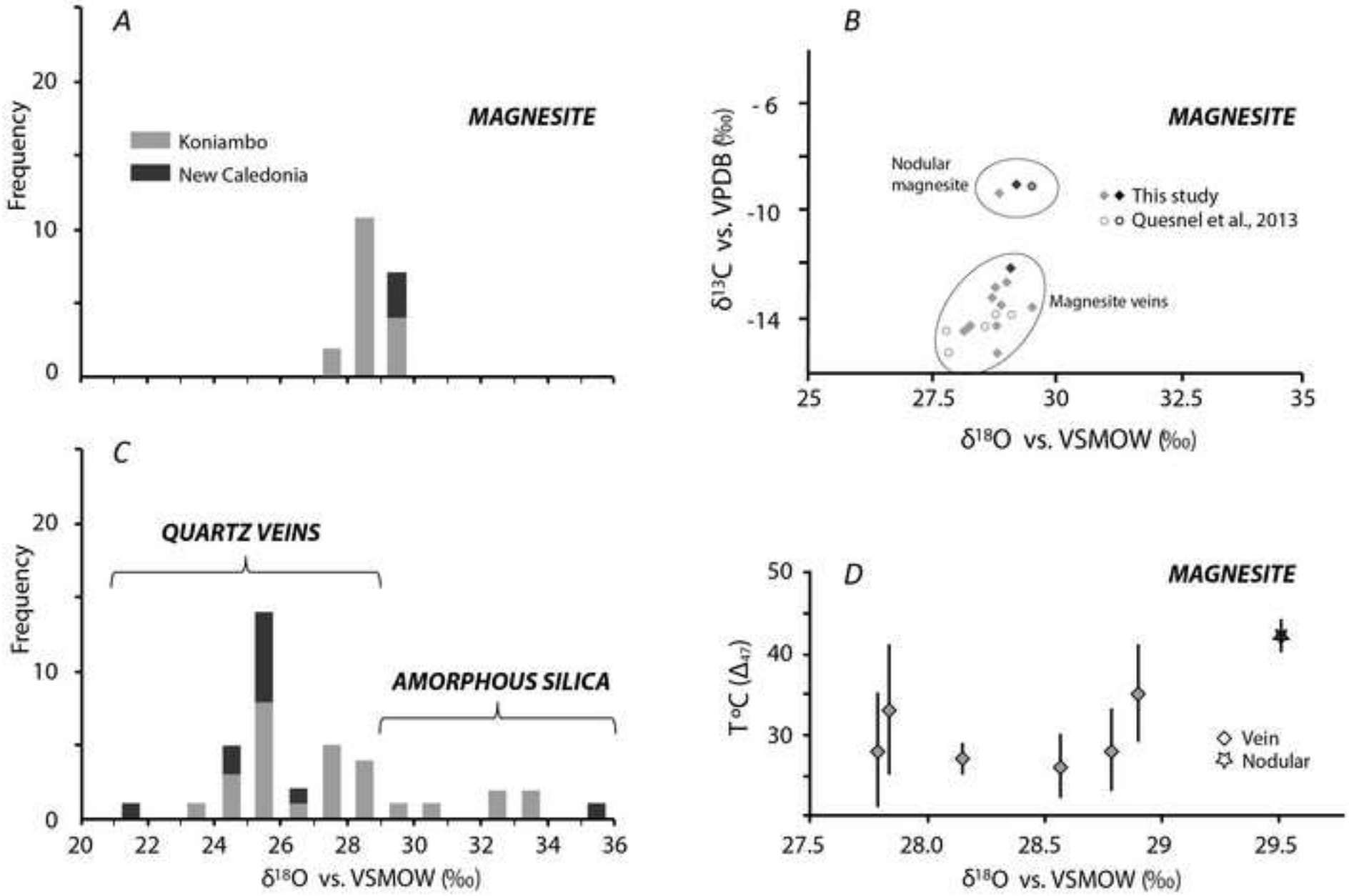

			Silica	Magnesite							
Sample	**Localization**	**Nature**	**$\delta^{18}O$**	**$\delta^{18}O$**	**$\delta^{13}C$**	**$\Delta^{18}O_{(Silica-Magnesite)}$**	**Δ_{47}**	**Standard error**	**T°C(Δ_{47})**	**n=**	**$\delta^{18}O$ fluid**
KONIAMBO MASSIF											
GBMS-Si-1	Koniambo 1: Sole	Magnesite vein+translucent opal	33.1	28.9	-13.5	4.2	0.671	0.016	35±6	3	-0.6
Bms Si 1'	Koniambo 1: Sole	Magnesite vein+translucent opal	32.9								
BMS Gio 15*	Koniambo 1: Sole	Magnesite vein+translucent opal	29.7	29.1	-13.8						
GBMS-2-13	Koniambo 1: Sole	Magnesite vein		28.3	-14.3						
GBMS-3-13	Koniambo 1: Sole	Magnesite vein		28.8	-14.3						
GBMS-4-13	Koniambo 1: Sole	Magnesite vein		29.0	-12.7						
GBMS-5-13	Koniambo 1: Sole	Magnesite vein		28.2	-14.3						
BMS Gio 9*	Koniambo 1: Sole	Magnesite vein		28.6	-14.3		0.695	0.012	26±4	3	-3.1
BMS Gio 3*	Koniambo 1: Sole	Magnesite vein		28.8	-13.8		0.689	0.016	28±5	4	-2.4
BMS Gio 12*	Koniambo 1: Sole	Magnesite vein		27.8	-15.2		0.675	0.024	33±8	3	-2.2
GVAV-1-13	Koniambo 2: Sole	Magnesite vein		28.7	-13.2						
GVAV-2-13	Koniambo 2: Sole	Magnesite vein		28.8	-15.3						
VAV Gio 9*	Koniambo 2: Sole	Magnesite vein		27.8	-14.4		0.691	0.020	28±7	4	-3.4
GMAR-2	Koniambo 3: High. Serp.	Magnesite vein		28.2	-14.5		0.693	0.006	27±2	2	-3.2
GMAR-3	Koniambo 3: High. Serp.	Magnesite vein		28.8	-12.8						
GMAR-5	Koniambo 3: High. Serp.	Magnesite vein		29.5	-13.6						
GMAR-4	Koniambo 3: High. Serp.	Nodular magnesite in soil		29.5	-9.1						
CR-1	Koniambo 3: High. Serp.	Nodular magnesite in soil		28.9	-9.4						
KNB3a	Koniambo: Saprolite	Qz	25.0								
MG1a	Koniambo: Saprolite	Qz	25.9								
MG3c	Koniambo: Saprolite	Qz	28.3								
MG5a	Koniambo: Saprolite	Qz	24.6								
FQZ 1	Koniambo 7: Saprolite	Qz	25.9								
Qz pim 1	Koniambo 7: Saprolite	Qz	26.0								
BAV Qz 1	Koniambo 7: Saprolite	Qz	25.9								
Si j 3	Koniambo 9: Saprolite	Qz	29.0								
Si Cl 3	Koniambo 9: Saprolite	Qz	28.1								
Si Cl Br 1	Koniambo 9: Saprolite	Qz	28.5								
FQZ 2	Koniambo 10: Saprolite	Qz	25.4								
Si Cl 1	Koniambo 10: Saprolite	Qz	27.5								
Si Cl 2	Koniambo 10: Saprolite	Qz	26.5								
Si j 4	Koniambo 11: Saprolite	Qz	28.0								
Test Pit	Koniambo 8: Saprolite	Mic Qz	25.1								
KNB3b	Koniambo: Saprolite	Mic Qz	27.6								
Si br 4	Koniambo 6: Saprolite	Mic Qz	23.9								
Pit 207 haut	Koniambo 7: Saprolite	Mic Qz	25.3								
Kon Bas Test Pit	Koniambo 8: Saprolite	Mic Qz	25.1								
Si br 6	Koniambo 9: Saprolite	Mic Qz	27.5								
Si br 2	Koniambo 10: Saprolite	Mic Qz	27.2								
Si R 1	Koniambo 10: Saprolite	Mic Qz	24.8								
BMS Si 13 2	Koniambo 1: Sole	Brown opal	33.4								
Si brune late	Koniambo 4: High. Serp.	Brown opal	32.6								
Conv Si 1	Koniambo 4: High. Serp.	Brown opal	30.4								
NEW CALEDONIA											
FOUE Gio	Foué peninsula	Magnesite vein		29.1	-12.1						
Bellevue Gio 1	Koné	Nodular magnesite in soil		29.2	-9.1						
DECH 1*	Koné	Nodular magnesite in soil		29.5	-9.1		0.652	0.005	42±2	3	1.5
NEP 4	Nepoui	Opal	35.3								
MONEO	Monéo	Mic Qz	26.3								
Thio SP5	Thio Plateau	Mic Qz	21.8								
"Fausse cargneule"	Thio Plateau	Qz	24.9								
BLV3 a	Thio Plateau	Qz	25.2								
3TX1 a	Thio Plateau	Qz	24.5								
Th Pl 3	Thio Plateau	Qz	25.1								
Th Pl 6	Thio Plateau	Qz	25.9								
Th Pl 9	Thio Plateau	Qz	25.8								
Th Pl 10	Thio Plateau	Qz	25.4								
Th Pl 11	Thio Plateau	Qz	25.5								